Measurement of tectonic surface uplift rate in a young collisional mountain belt

Lon D. Abbott*†, Eli A. Silver*, Robert S. Anderson*, Randall Smith‡, James C. Ingle§, Stanley A. Kling‖, David Haig¶, Eric Small*, Joseph Galewsky* & William Sliter#

* *Department of Earth Sciences, University of California, Santa Cruz, California 95064, USA*
‡ *GeoInformation Technology, 2771 E. Shaw Avenue, Fresno, California 93710, USA*
§ *Department of Geological and Environmental Sciences, Stanford University, Stanford, California 94305, USA*
‖ *416 Shore View Lane, Leucadia, California 92024, USA*
¶ *Department of Geology and Geophysics, University of Western Australia, Nedlands, Perth, Western Australia 6009, Australia*
# *United States Geological Survey, Western Geologic Mapping Team—Mail Stop 975, 345 Middlefield Road, Menlo Park, California 94025, USA*

Measurement of the rate of tectonically driven surface uplift is crucial to a complete understanding of mountain building dynamics. The lack of a suitable rock record typically prevents determination of this quantity, but the unusual geology of Papua New Guinea's Finisterre mountains makes measurement of this rate possible. The tectonic surface uplift rate at the Finisterre range is 0.8–2.1 mm yr^{-1}, approximately that expected to arise from crustal thickening.

In the study of mountain belts, one of the most fundamental quantities that geoscientists seek to measure is the uplift rate. The term 'uplift' is often loosely applied and may refer to one of several distinct quantities[1]. Among the most important types of uplift are: rock uplift, tectonic uplift at a point, exhumation, and tectonic surface uplift. Rock uplift is the total displacement of a point of rock with respect to sea level (or the geoid). Rock uplift can be driven by tectonic forces or by the isostatic response to erosion. Tectonic uplift at a point is that portion of rock uplift that is driven exclusively by tectonics. Exhumation is the sum of erosion and tectonic denudation. It tracks the displacement of rocks towards the Earth's surface, so, unlike rock uplift and tectonic uplift, which are referenced to sea level, exhumation measurements do not record elevation changes. Tectonic surface uplift is the mean displacement (relative to sea level or the geoid) of a broad region (over 1,000 km^2) of the Earth's surface resulting solely from tectonic activity[1]. Stated another way, tectonic surface uplift is the mean tectonic uplift for all points within an area larger than 1,000 km^2.

The importance of tectonic surface uplift lies in its utility for quantifying large-scale tectonic forces. Measurement of rock uplift or tectonic uplift at individual points yields information about local structures. However, because tectonic processes operate at crustal scales, it is average tectonic uplift over a broad area (tectonic surface uplift) that is needed to quantify the tectonic forces responsible for mountain building[1]. Measurement of the tectonic surface uplift rate (TSUR) can help illuminate the mechanics of mountain building and provide important constraints on the behaviour of the continental lithosphere[1,2]. For instance, although the main tectonic mechanism driving the growth of mountain ranges is thickening of the continental crust during plate collision[3], several additional tectonic uplift mechanisms have been proposed[2,4,5]. If supplementary mechanisms have contributed to unusually rapid uplift, the measured TSUR should exceed the rate expected from crustal thickening. Whether mountains can rise faster than is possible via crustal thickening is central to the recent debate over whether rapid uplift of Tibet caused late Cenozoic climate change[6–8]. The TSUR also provides an important constraint for numerical models that explore dynamic feedbacks between lithospheric and surface processes during mountain building[9,10].

† Present address: Down To Earth Technology, 2964 Palo Parkway, Boulder, Colorado 80301, USA.

Despite its importance to modern quantitative tectonic studies, the TSUR is so difficult to quantify that it has never been successfully measured[1]. Most uplift studies measure rock uplift (for example, geodetic surveys) or exhumation (for example, thermochronological studies). Valuable information is gleaned from these techniques, but because they do not measure TSUR, they cannot be used to quantify large-scale tectonic forces[1].

Here we show that the unusual geology of Papua New Guinea's Finisterre mountains (Fig. 1) allows quantification of the TSUR. Limestone plateaux, whose surfaces have suffered little or no erosion, provide uplift markers. Using biostratigraphic methods, we dated the surface rocks and determined their depositional water depth at 15 plateau-top control points. We then fitted a continuous surface to the pleateaux and assigned each surface point an age and water depth by interpolating from the control points. Subtracting the present topography from the reconstructed surface yielded an erosion map, from which we calculated the isostatically driven rock uplift at each point that can be attributed to erosional unloading. The tectonic component of uplift for each point was derived by subtracting this isostatic uplift component from the total rock uplift. Finally, we calculated the TSUR by dividing the magnitude of tectonic uplift by the uplift duration at each point and averaging these values over all points on the surface.

The TSUR for the central Finisterre range is between 0.8 and 2.1 mm yr^{-1}. The uplift rate expected to be caused by crustal thickening is 0.6–3.0 mm yr^{-1}. The TSUR is therefore consistent with crustal thickening being the only cause of uplift, but the existence of additional mechanisms that either increase or retard uplift is not precluded. The Finisterre TSUR is also similar to the average rock uplift rate for Quaternary terraces along the range's northeastern coast[11,12]. This similarity offers hope that data on terrace rock uplift may provide a proxy for the TSUR in some areas lacking the conditions necessary to measure the latter.

Measurement of the TSUR

The total uplift at a point, i, can be expressed as follows[13,14] (Fig. 2):

$$U_i = (Z_i - Z_{0_i}) + E_i + \Delta H_{\mathrm{sl}_i} \quad (1)$$

where, at any point i, U_i is the total uplift, Z_i is the present topographic elevation, Z_{0_i} is the original topographic elevation

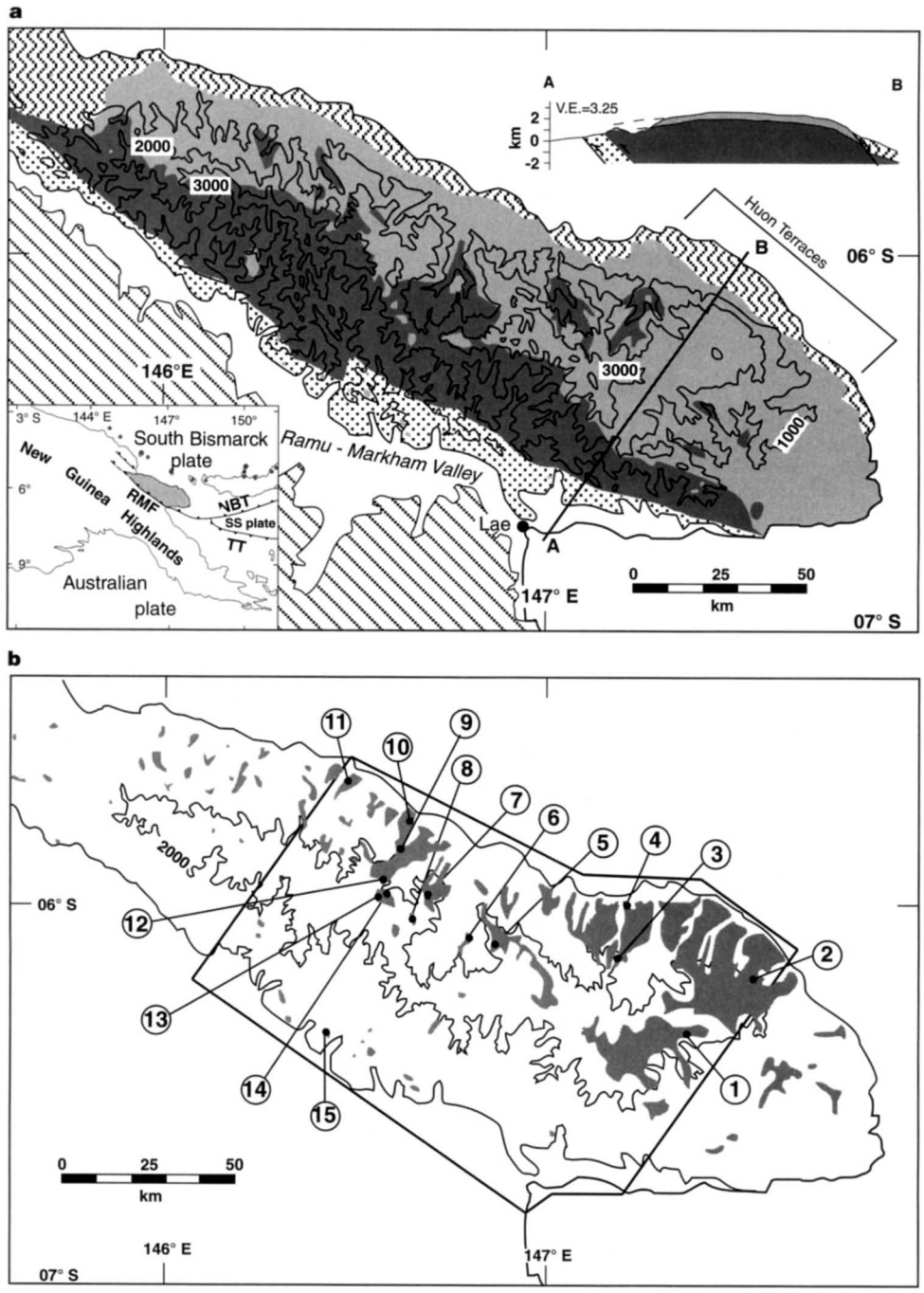

Figure 1 **a**, Simplified geological map of the Finisterre range with 1,000-m elevation contours. The Ramu–Markham Valley marks the collision suture. Patterns are as follows. Dark shading, Oligocene to Early Miocene volcanic and volcaniclastic rocks; light shading, Gowop Group marine carbonate rocks; stippling, Neogene and Quaternary clastic accretionary wedge; wave pattern, other Finisterre terrane rocks; hatching, New Guinea Highlands. Cross-section A–B illustrates the anticlinal nature of the range. The Finisterre range is shaded on the inset map showing the tectonic setting of the Finisterre arc–continent collision. RMF, Ramu–Markham fault (the collision suture); NBT, New Britain trench; SS plate, Solomon Sea plate; TT, Trobriand trough. **b**, Outcrops of Gowop Group rocks used to reconstruct the zero-erosion surface are shaded on this map of the Finisterre range. In places, the Gowop Group mapped in **a** is heavily dissected. Only outcrops displaying little or no erosion, as evidenced by their plateau morphology and Nokopo Formation composition (the youngest unit of the Gowop Group), are used in the reconstruction and hence shaded here. A few of the smallest shaded areas are ridgetop outcrops of Gowop Group too small to show plateau morphology but they mark sites of modest or no erosion in otherwise heavily dissected areas. Plateau outlines were digitized from a digital elevation model that was constructed on a 55-m grid from 1:100,000 scale topographic maps using the TNTMips software. Numbers 1–15 mark the control points used in the TSUR calculation. Age and elevation data for these points are in Table 1. The 2,000-m elevation contour is shown. The bold outline surrounds the 12,000 km^2 region for which the TSUR calculation was done.

with respect to sea level at the time of formation, E_i is the thickness of eroded material, and ΔH_{sl_i} is the change in sea level (with a sea-level rise from the time of creation of the marker to the present assumed to be positive).

Uplift at a point can be driven by tectonics or by the isostatic response to exhumation. Some portions of any landscape are being eroded more rapidly than others, with erosion rate variations occurring over distances of metres to kilometres. In contrast, the isostatic response to erosion is regional; the lithosphere responds to the average amount of erosion over an area 10^4 km^2 or more[15]. Hence, areas that are eroding more slowly than the regional average will be displaced upwards (relative to sea level), even in the absence of tectonic forcing[1,16]. The total uplift at a point can be expressed as the sum of its tectonic and isostatic components:

$$U_i = U_{t_i} + U_{e_i} \quad (2)$$

where, at the point i, U_{t_i} is the tectonic component of uplift and U_{e_i} is the erosionally induced isostatic component of uplift.

An expression for the tectonic component of uplift at point i can be derived[13,14] by combining equations (1) and (2) and solving for U_{t_i}:

$$U_{t_i} = (Z_i - Z_{0_i}) + E_i + \Delta H_{sl_i} - U_{e_i} \quad (3)$$

The rate of tectonic uplift at point i is calculated by dividing this tectonic uplift expression by the duration of uplift, t_i:

$$\text{rate of tectonic uplift of point } i = \frac{U_{t_i}}{t_i} \quad (4)$$

To be meaningfully applied to large-scale tectonic problems, the tectonic uplift rates calculated (from equation (4)) at all points on a surface greater than 1,000–10,000 km^2 must be averaged to obtain the TSUR[1]:

$$\text{TSUR} = \frac{1}{N}\sum_{i=1}^{N}\left[\frac{(Z_i - Z_{0_i}) + E_i + \Delta H_{sl_i} - U_{e_i}}{t_i}\right] \quad (5)$$

where N is the number of sample points.

Examination of equation (5) makes it clear that measurement of the TSUR requires the following: (1) Preservation of a datable rock sequence that was deposited during or immediately before uplift (to constrain t); (2) a record of depositional elevation for that rock sequence (to constrain Z_0); (3) measurement of the erosional thickness (E) at every point and knowledge of the original density of the missing material (to calculate U_e); and (4) knowledge of the change in sea level between the time of deposition and the present.

The geological record in most areas is too incomplete to satisfy all the above constraints. The syn-orogenic sediments that meet requirement (1) are usually quickly eroded. On high plateaux these sediments are often preserved, but most are deposited above sea level, making it difficult to determine their depositional elevation (requirement (2)). Finally, it is rare to find surfaces experiencing no erosion within mountain ranges. Without such reference points, the total amount of eroded material (requirement (3)) is difficult to quantify.

Application to the Finisterre range

The Finisterre mountains formed 3.0–3.7 Myr ago in response to collision between the Finisterre volcanic arc terrane and the Australian continental margin[17]. Oligocene and Early Miocene volcanic and volcaniclastic rocks of the Finisterre arc are overlain unconformably by a sequence of Neogene and Quaternary marine carbonate rocks (the Gowop Group)[18]. This sequence is broadly folded and thrust over clastic rocks of a Neogene accretionary wedge (Fig. 1)[19,20]. The broad anticline forming the range has been eroded into a series of high plateaux separated by deep gorges.

The Finisterre range possesses all of the attributes necessary for determination of the TSUR. The plateaux are capped by marls deposited during collision whose age and original depth of deposition can be determined (requirements (1) and (2)), and the plateau tops are zero-erosion surfaces that provide reference points for the thickness of eroded material in the gorges (requirement (3)). Finally, ΔH_{sl_i} can be obtained from eustatic sea-level curves (requirement (4)).

Table 1 Data for each control point on the plateau surface

Control point	Age (Myr)	Original water depth (m)	Modern elevation (m)	ΔH_{sl} (m)	U_r (mm yr^{-1})
1	3.0–3.1	500–2,000	2,460	−60 to +70	0.9–1.5
2	0.95–1.7	1,600–2,000	1,870	−20 to +90	2.0–4.2
3	2.55–2.7	2,000–3,000	2,040	−20 to +90	1.5–2.0
4	1.0	2,000–3,000	210	−20 to +85	2.2–3.3
5	3.0–5.2	150–3,000	2,400	−90 to +95	0.4–1.8
6	4.0	1,200–2,000	1,840	−70 to +55	0.7–1.0
7	1.7–1.9	150–500	2,530	−20 to +90	1.4–1.8
8	3.0–3.8	500–2,500	2,470	−70 to +80	0.8–1.7
9	3.6–4.2	150–3,000	1,500	−90 to +80	0.4–1.3
10	3.0–3.1	150–3,000	410	−60 to +70	0.2–1.2
11	0.95–1.7	50–100	140	−20 to +90	0.1–0.4
12	2.7	1,500–3,000	2,500	+20 to +90	1.5–2.1
13	1.1–1.8	0–150	2,620	−20 to +90	1.4–2.6
14	2.4–2.6	1,200–2,500	2,450	−20 to +100	1.4–2.1
15	1.0–2.0	500–2,000	680	−20 to +90	0.6–2.8

Control point locations are shown in Fig. 1b. Age ranges are based on palaeontological zonations calibrated to the most recent timescale of Berggren *et al.*[36,37]. The uncertainty in the age determined for a given sample is a function of the preservation and diversity of its microfossil biota and the stratigraphic range of that biota. Samples listing a single age either contain a biota diagnostic of a well-dated biostratigraphic event or are assigned an age by extrapolation from well-dated samples lower in the section by assuming a constant rate of sediment accumulation. Original water depths are calibrated using the classification of Ingle[38]. Modern elevation is the present sample elevation, ΔH_{sl} is the sea level change from the time of deposition to the present[30], and U_r is the rock uplift rate at each control point.

The age of the plateaux. Marls of the Nokopo Formation, the youngest unit of the Gowop Group[18], cap most of the plateaux. The marls contain benthic and planktonic foraminifera and calcareous nannoplankton that we dated using biostratigraphic methods. We examined 207 Nokopo Formation samples from 20 sites throughout the central Finisterre range. Only samples from the formation's stratigraphic top were used to constrain plateau ages. Samples from 15 sites yielded useful age information (Fig. 1b, Tables 1 and 2).

Determination of any post-depositional erosion of the plateau surfaces is crucial. If erosion has occurred, the values used for E_i and U_{e_i} in equation (5) will be too low and those used for t_i will be too high, making the calculated TSUR a minimum. Several lines of evidence suggest that erosion has been minimal. (1) Porosities in plateau-top Nokopo Formation outcrops are commonly ⩾50% (L.D.A., unpublished data); such high porosities would not be maintained if the samples have been buried more than a few tens of metres (ref. 21). (2) The soft, easily erodable Nokopo Formation caps most plateaux that we visited. As in most areas the formation is 50–100 m thick[18], only a small amount of erosion would strip the unit from the plateaux. (3) Modern plateau erosion is dominated by the formation of karst dolines, leaving much of the surface intact. (4) The gentle dips of most Nokopo Formation outcrops are concordant with the dip of the plateau surface; erosional plateaux often display discordance. (5) A low vitrinite reflectance (R_0) value of 0.15% was obtained near the base of an anomalously thick (623 m) Nokopo Formation section, indicating that the sample has not been exposed to temperatures >65 °C (M. Bustin, personal communication). Such extreme thermal immaturity precludes substantial erosion[22].

Examination of Table 1 shows that the plateau surface ages differ

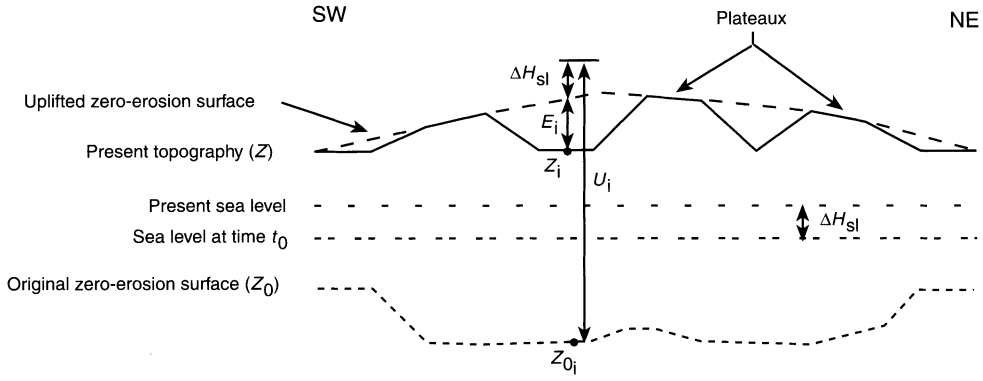

Figure 2 Schematic cross-section of Finisterre range uplift illustrating the quantities used in the TSUR calculation. A depositional surface originally below sea level (Z_0, short dashed line) was uplifted and eroded to form the present topography (Z, solid line). U_i is the total uplift at point i. Plateaux preserve part of the original surface, but erosion (E_i) has formed canyons elsewhere. The long dashed line connecting the plateaux reconstructs a surface of zero erosion. ΔH_{sl} is the change in sea level between time t_0, when surface Z_0 was formed, and today.

by as much as three to four million years. It is possible that this diachrony indicates erosion at some control points; however, diachrony of the zero-erosion surface is expected because uplift of the range has progressed from northwest to southeast[17,23] and because the range has been uplifted as a broad dome rather than uniformly. Turbidite sediments would bypass the dome's rapidly rising uplift axis sooner than they would the more gently rising dome flanks, causing diachrony of the zero-erosion surface and helping to explain both the variable thickness of the Nokopo Formation and the lack of accumulation of younger, shallower-water sediments later in the submarine uplift phase. Bottom currents may also have prevented accumulation of younger hemipelagic sediments. The ages of plateau-top samples are consistent with the direction and timing of collision propagation[17,23], and with the expectation of younger ages on the dome's flanks.

The original elevation of the pleateau-top marls. The original depositional water depth for each Nokopo Formation sample was deduced from benthic foraminifera. Most of the benthic foraminifera identified in our samples are still living in the southwestern Pacific Ocean and their established modern depth ranges in this region were used to interpret original depth of deposition. The depth ranges shown in Table 1 reflect the maximum and minimum possible depths of deposition. The species used in the depth determination for a representative sample are shown in Table 2.

Determination of the depositional water depth produces the single largest source of uncertainty in the TSUR calculation because most of the Nokopo Formation was deposited at lower bathyal to lower middle bathyal oceanic depths, the region including the broadest depth ranges exhibited by modern species (1,500–4,000 m depth). However, specimens of deeper dwelling species in

Table 2 Microfossils identified at control point 2

Calcareous nannoplankton	Planktonic foraminifera	Benthic foraminifera
Calcidiscus macintyrei (F)	*Candeina nitida*	*Cassidulina* sp.
Cyclicargolithus floridanus (R)	*Globigerinella aequilateralis*	*Cassidulina crassa*
Dictyococcites antarcticus (V)	*Globigerinoides ruber*	*Ceratobulimina pacifica*
Dictyococcites minutus (A)	*Globigerinoides conglobatus*	*Cibicidoides bradyi*
Dictyococcites productus (F)	*Globigerinoides sacculifer*	*Fissurina* sp.
Discoaster assymetricus (R)	*Globorotalia hirsuta*	*Globocassidulina subglobosa*†
Discoaster brouweri (R)	*Globorotalia menardii*	*Hoeglundina elegans*
Discoaster deflandrei (V)	*Globorotalia scitula*	*Laticarinina pauperata*
Discoaster surculus (R)	*Globorotalia tumida*	*Melonis pompilioides*†
Emiliania annula (F)*	*Globorotalia tosaensis tenutheca**	*Nodosaria* sp.
Gephyrocapsa (small) (C)*	*Globorotalia truncatulinoides**	*Oridorsalis tener*
Helicosphaera carteri (C)	*Neogloboquadrina dutertrei*	*Oridorsalis umbonatus*†
Helicosphaera sellii (F)*	*Orbulina universa*	*Planulina wuellerstorfi*†
Pontosphaera spp. (V)	*Pulleniatina obliquiloculata**	*Pleurostomella* sp.
Reticulofenestra minuta (A)		*Pyrgo murrhina*
Reticulofenestra minutula (C)		*Quinquiloculina* sp.
Reticulofenestra pseudoumbilica (R)		*Sigmoilopsis schlumbergi*
Sphenolithus moriformis (F)		*Stilostomella* sp.
Thoracosphaera sp. (R)		*Uvigerina hispida*†
		Valvulineria sp.

* Key planktonic foraminifera and nannoplankton species for age determination.
† Key benthic species for estimating depth of deposition.
V, very rare (1 specimen); R, rare (2–10 specimens); F, few (11–100); C, common (101–1,000); A, abundant (>1,000).

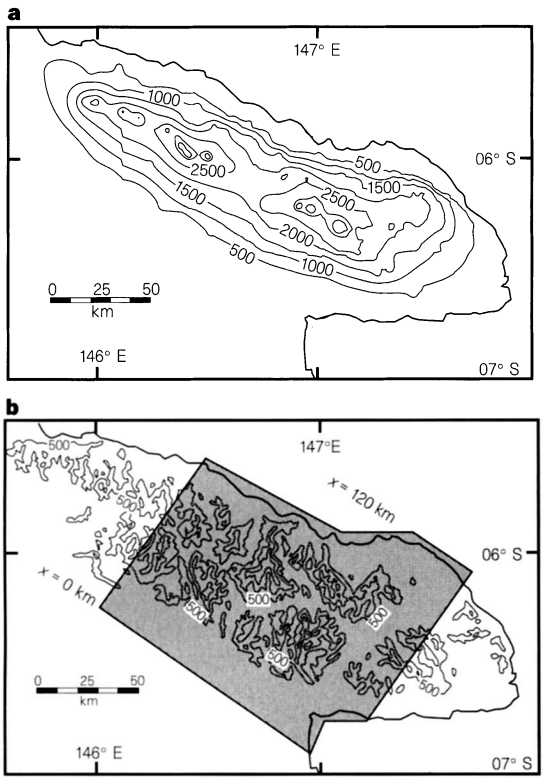

Figure 3 a, Contour map of the zero-erosion surface. The plateaux shown in Fig. 1b were imported to the Geographical Resource Analysis Support System (GRASS) software, where a regularized spline was fitted to them. A high tension of 300 was used to produce a surface that stretches tautly between extant plateaux[24,25]. Contour interval is 500-m. **b**, Map of erosion height with 500-m contour interval. The map was generated by subtracting the existing topography (Fig. 1a) from the reconstructed depositional surface (**a**). The shaded area shows the TSUR calculation space, which is also the region used to produce the mean erosional profile of Fig. 4a. The $X = 0$ line marks the collision suture in the Ramu-Markham Valley. The Australian plate may be broken at the $X = 120$ km line[26].

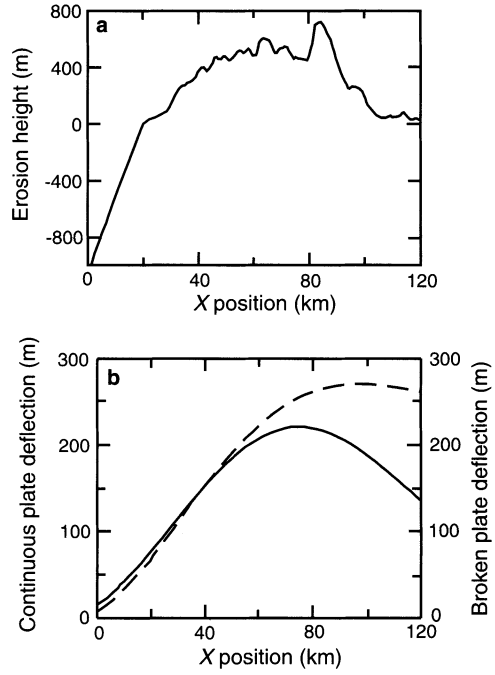

Figure 4 a, Profile of erosion thickness across the range (from $X = 0$ to $X = 120$ km, see Fig. 3b), constructed by averaging the erosion height along a swath 140 km wide (Fig. 3b) parallel to the strike of the range. Deposition in the Ramu-Markham Valley (Fig. 1a) also causes flexure, and is shown as a negative erosion height. The valley's sedimentary section thickens southwestwards from 300 m near the range front to about 1,000 m near the southern edge[39]. **b**, Profiles of erosionally driven uplift (U_{e_i}) at each point due to the erosional load profile shown in **a**, for both a continuous plate (solid line) and a plate broken at $X = 120$ km (dashed line, see Fig. 3b). The calculations follow Small and Anderson[16] and assume: effective elastic thickness = 20 km; Poisson's ratio = 0.25; Young's modulus = 7×10^{10} Pa; flexural rigidity = 5×10^{22} N m. The flexural model is a one-dimensional approximation for the response to a two-dimensional erosion pattern (Fig. 3b). A test of the calculation's sensitivity to this approximation is to vary the swath width along which erosion is averaged in **a**. If the one-dimensional approximation is insufficient, then the U_{e_i} values obtained using a narrow swath will differ significantly from those obtained using a wide swath. The maximum difference in U_{e_i} at any single point for swath widths between 10 km and 190 km is small (±25 m for a continuous plate and ±38 m for a broken plate), justifying the one-dimensional approximation.

control samples lack the corrosion that is common to foraminifera deposited at or approaching the carbonate compensation depth, restricting their maximum water depth to <3,000 m.

A much smaller uncertainty arises in determination of the present sample elevation. Elevation was determined using barometric altimetry and by locating samples on 1:100,000 scale topographic maps with 40-m contour intervals. The average elevation uncertainty is ±35 m.

Reconstruction of the zero-erosion surface. Finisterre plateaux on opposite sides of deep river gorges lie at nearly identical elevations, indicating that they are remnants of an originally more extensive surface. We reconstructed this zero-erosion surface by generating a digital elevation model, on which we digitized the outlines of the existing plateaux (Fig. 1b). Fitting a continuous surface to the plateaux (Figs 2, 3a) was done using a regularized spline with adjustable tension that can handle irregularly spaced data[24,25]. By subtracting the present topography from the reconstructed surface, we produced an erosional thickness (E_i) map (Fig. 3b), which is needed to calculate the magnitude of erosionally induced uplift (U_{e_i}).

Mistakes in reconstruction of the zero-erosion surface would cause errors in the erosion thickness map and therefore in the erosionally driven uplift component (U_{e_i}). Although we cannot assign quantitative uncertainties to the surface misfit, we believe it to be small. The reconstruction (Fig. 3a) provides a good fit to the existing plateau on the Huon peninsula, where it forms a nearly intact, broad arch (Fig. 1). Plateau surfaces are extensive and closely spaced on the northeast flank of the range (Fig. 1b), minimizing fitting errors here. Plateaux are rare along the southwest flank of the range, but a few small, widely distributed outcrops of the Gowop Group, which immediately underlies the plateaux elsewhere, strongly constrain acceptable surface fits. The broad anticline forming the Finisterre range is disrupted by smaller folds and faults[20]. However, these are low-amplitude, second-order complications that do not cause significant errors in the surface reconstruction.

The magnitude of erosional uplift. Knowing the distribution of erosion (Fig. 3b), it is possible to calculate the magnitude of erosionally induced uplift (U_{e_i}) at each point. The flexural rigidity of the lithosphere in the Finisterre collision zone is between 1×10^{22} and 2×10^{23} N m (refs 26, 27). At such rigidities, isostatic compensation of the 80–120 km wide Finisterre range will be regional.

Using the method of Hetenyi[28], we constructed a one-dimensional elastic flexure model to calculate the deflection field (U_e) that would result from the Finisterre erosion pattern. The erosional load used in the model is a range-normal profile of average erosional thickness across a swath 140 km wide (Fig. 4a).

Figure 4b depicts the flexural response (U_e) to the erosional load profile of Fig. 4a. The Australian plate may be broken near the northern edge of the Finisterre range (Fig. 3b)[26], but an enigmatic plane of seismicity at about 100 km depth leaves the mechanical nature of the lithosphere under the Finisterre range uncertain[29]. Given this uncertainty, we performed U_e calculations for both continuous and broken plate models, assuming an intermediate flexural rigidity of $D = 5 \times 10^{22}$ N m. Using the published endmember values for D produces a maximum uncertainty in U_{e_i} of ± 85 m for a continuous plate and ± 75 m for a broken plate. Our one-dimensional approximation results in only small uncertainties because the lithosphere responds to regional erosion, reducing the effect of local erosional thickness variations (Fig. 4b).

Calculation of palaeo sea level. Conflicting eustatic sea-level curves have been published for the time period (1–4 Myr ago) of Nokopo Formation deposition, and rapid (10^4–10^5 yr) oscillations in sea level that have occurred since the Pliocene are not accounted for in all curves[30]. We used the endmember values of published sea-level curves[30–32] for the ΔH_{sl_i} range at each control point (Table 1).

Calculation of the tectonic surface uplift rate. We gridded the digital elevation model at 1-km intervals and assigned every grid point values for each parameter in equation (5). This involved interpolation of age and depositional depth data between control points. It is difficult to quantify the uncertainties associated with this interpolation, but abrupt age discrepancies (apart from the systematic diachrony discussed above) are unlikely, given that the tectonic and oceanographic controls on deposition would be similar throughout the area. It is also unlikely that major bathymetric ridges with enough relief to affect our calculations have gone undetected, given the control point spacing.

To calculate the TSUR, we applied equation (5) to all gridded points in a 12,000 km^2-calculation space that includes both remnants of the zero-erosion surface and areas dissected by erosion (Figs 1b, 3b). The calculation space is large enough to provide a meaningful TSUR[1]. The calculation was run for both continuous and broken plate models. The maximum possible TSUR was calculated using the youngest sample age, deepest original depth, lowest palaeo sea level, and smallest erosional uplift component. The minimum possible TSUR was calculated using the antithetic endmember values for each parameter. The TSUR is 0.86–2.06 mm yr^{-1} for a continuous plate and 0.84–2.03 mm yr^{-1} if the plate is broken.

All quantifiable uncertainties have been included in the calculations. The most significant of these are the depositional depth, which can be as much as 2,950 m for a given sample, and the sample age, which can be as great as 2.2 Myr. Provided that the plateau surfaces do represent surfaces of zero erosion and that our reconstruction of the original zero-erosion surface is accurate, uncertainties stemming from all other aspects of the calculation are relatively small (at most 432 m for a given point). The TSUR is clearly not sensitive to whether the Finisterre lithosphere behaves as a continuous or a broken plate.

Implications of the calculated TSUR

Because our study is the first to calculate the TSUR, it allows the first comparisons to be made between that rate and other measures of uplift. Rock uplift rates of 2.0–7.6 mm yr^{-1} have been measured over the past 21 kyr at several locations in the Ramu–Markham Valley (Fig. 1a), the collision suture zone[33]. A suite of coastal coral terraces on the Huon peninsula (Fig. 1a) display rock uplift rates over the past 340 kyr decreasing from 3.0 to 0.5 mm yr^{-1} away from the suture zone[11,12]. The average rock uplift rate for the terraces, derived from a contour map of uplift rates[11], is approximately 1.5 mm yr^{-1}, similar to the 0.8–2.1 mm yr^{-1} TSUR. These results suggest that, although individual rock uplift rates are not indicative of the TSUR, the average rock uplift rate for the terraces does offer a reasonable approximation of the TSUR. Quaternary coastal terraces are the only extensive, datable surfaces in many mountain ranges. Although our results pertain only to the Finisterre range, the similarity between the average terrace rock uplift rate and the TSUR suggests that where rock uplift rates can be averaged across extensive constructional coastal terrace suites, this rate may provide a reasonable proxy for the TSUR.

The method used here for measuring the TSUR illustrates the many issues that must be addressed if tectonically meaningful uplift rates are to be determined. These issues are particularly important for models that attempt to unravel dynamic feedbacks between listhospheric and surface processes during mountain building[9,10]. These feedbacks can be misrepresented if measured rock uplift rates are used instead of the TSUR; the rock uplift rates are themselves manifestations of these feedbacks because they result from a combination of both tectonic and erosional processes.

Knowing the TSUR, we may determine whether crustal thickening explains the rate of rise. Uplift caused by crustal thickening can be estimated using either an isostatic balance between normal and crustally thickened lithosphere, or by modelling the range as a fault bend fold formed over a crustal-scale fault ramp. Both methods require some input parameters that are poorly constrained for the Finisterre collision.

The first method uses an equation for the surface elevation difference (Δe) between crustally thickened and normal columns of lithosphere[2]:

$$\Delta e = (S - S_0)\left(\frac{\rho_{m0} - \rho_{c0}}{\rho_a}\right) - \frac{\alpha T_1}{2L} \times \left[\left(\frac{\rho_{m0} - \rho_{c0}}{\rho_a}\right)\left(\frac{S^2}{\gamma} - S_0^2\right) + \frac{\rho_{m0}}{\rho_a}(\gamma - 1)L^2\right]$$

where ρ_{m0} is the 0 °C density of the mantle (3,330 kg m^{-3}), α is the volume coefficient of thermal expansion (3.4×10^{-5} K^{-1}), T_1 is the temperature at base of lithosphere (1,333 °C), S is the present crustal thickness, S_0 is the crustal thickness before collision, L is lithospheric thickness in an unstrained state, ρ_a is the asthenosphere density = $\rho_{m0}[1 - \alpha T_1] = 3{,}179$ kg m^{-3}, ρ_{c0} is the crustal density, and $\gamma = S/S_0$, the crustal thickening factor. The values cited for ρ_{mo}, α and T_1 are taken from England and Houseman[2]. The crustal thickness of the Finisterre collision zone is not well constrained, but L.D.A. *et al.*[20] estimated $S = 52$ km and $S_0 = 37$ km. As the lithospheric thickness has not been measured, we performed calculations for a span of reasonable values ($L = 80$–120 km). Following England and Houseman[2], the crustal density was chosen such that the initial continental column is in isostatic balance with a standard mid-ocean ridge column, but we modified the initial continental column used by those authors to consist of between 775 and 2,115 m of water overlying continental crust. This initial column reflects conditions in the Finisterre area before collision and results in $\rho_{c0} = 2{,}692$–$2{,}855$ kg m^{-3}. For lithospheric thicknesses between 80 and 120 km, Δe is in the range 1,450–1,840 m. Uplift began in the southwestern portion of the study area about 2.5–3.0 Myr ago and in the northeastern portion about 1.0–1.5 Myr ago[17,23]. Dividing these elevation change values by the duration of uplift in each area yields average uplift rates due to crustal thickening of 0.6–1.3 mm yr^{-1}.

Alternatively, the range can be modelled as a fault bend fold[3]. The Finisterre range is an anticline formed above a terrane-bounding fault[19,20] that appears from earthquake data to dip ~15° NE over most of its length and steepen near the suture zone[26,34]. If the convergence rate and ramp angle are known, then trigonometry can

be used to calculate the crustal thickening rate over the ramp. The advantage of this approach is that crustal and lithospheric thicknesses do not have to be specified; a drawback is that, because uplift rates are low in areas not moving up the ramp[3], the portion of the study area ascending the ramp at any given time must be estimated.

South Bismarck–Australian plate convergence is 82 mm yr^{-1} in the vicinity of the study area[35]. As much as 45 mm yr^{-1} of this convergence may be accommodated by deformation within the Australian plate itself[26], making the convergence rate across the Finisterre mountains 37–82 mm yr^{-1}. The rate of crustal thickening over a 15° fault ramp expected for these convergence rates is 9.6–21.2 mm yr^{-1}. Accounting for isostatic compensation, this crustal thickening rate would yield an uplift rate of 1.7–3.8 mm yr^{-1} over the fault ramp if the entire range were ascending the fault ramp throughout the collision. Given the convergence and collision propagation rates, it is more likely that the northeastern portion of the 80–120 km wide range reached the fault ramp 1–2 Myr after the leading (southwestern) edge of the range. Therefore, on average, each point in the study area was ascending the ramp for roughly 50–80% of the collision duration, resulting in an expected TSUR of 0.9–3.0 mm yr^{-1}.

The measured TSUR (0.8–2.1 mm yr^{-1}) and the expected uplift rates using both methods described above (0.6–1.3 mm yr^{-1} and 0.9–3.0 mm yr^{-1}) all agree over most of their respective ranges, supporting a conclusion that the Finisterre range is built solely by crustal thickening processes. However, the range in these data allows for the TSUR either to exceed the uplift rate expected due to crustal thickening, in which case additional uplift mechanisms must be sought[2,4,5], or to fall below the crustal thickening uplift rate. An unexpectedly slow TSUR could be caused by subsurface loads beneath the range[3], the presence of which is suggested by gravity data[26].

The TSUR provides an important constraint on subsurface processes that is not available for any other mountain range. Unfortunately, other critical data for the Finisterre range are currently lacking, making it difficult to determine whether the observed TSUR is the exclusive product of crustal thickening or if other processes are contributing to growth of the range. New studies are needed to better constrain such parameters as the range's crustal and lithospheric thicknesses and the convergence rate across the range. Used in conjunction with such new data, the TSUR could quantify the rates and magnitudes of the lithospheric processes responsible for range formation more fully than has been possible elsewhere. □

Received 17 January; accepted 18 December 1996.

1. England, P. & Molnar, P. *Geology* **18,** 1173–1177 (1990).
2. England, P. C. & Houseman, G. A. *J. Geophys. Res.* **94,** 17561–17579 (1989).
3. Molnar, P. & Lyon-Caen, H. in *Geol. Soc. Am. Spec. Publ.* **218,** 179–207 (1988).
4. Bird, P. *J. Geophys. Res.* **84,** 7561–7571 (1979).
5. Charlton, T. R. *Geology* **19,** 28–31 (1991).
6. Raymo, M. E., Ruddiman, W. F. & Froelich, P. N. *Geology* **16,** 649–653 (1988).
7. Molnar, P. & England, P. *Nature* **346,** 29–34 (1990).
8. Molnar, P., England, P. & Martinod, J. *Rev. Geophys.* **31,** 357–396 (1993).
9. Koons, P. O. *Am. J. Sci.* **289,** 1041–1069 (1989).
10. Beaumont, C., Fullsack, P. & Hamilton, J. in *Thrust Tectonics* (ed. McClay, K. R.) 1–18 (Chapman & Hall, 1992).
11. Chappell, J. *Geol. Soc. Am. Bull.* **85,** 553–570 (1974).
12. Chappell, J. *Search* **14,** 99–101 (1983).
13. Garfunkel, Z. *Tectonophysics* **150,** 33–49 (1988).
14. Brown, R. W. *Geology* **19,** 74–77 (1991).
15. Tsuboi, C. *Gravity* (George Allen & Unwin, 1983).
16. Small, E. E. & Anderson, R. S. *Science* **270,** 277–280 (1995).
17. Abbott, L. D. *et al. J. Sed. Res.* **B64,** 169–183 (1994).
18. Abbott, L. D. in *MARKHAM 1:250,000 Geological Series (Revision 1): Explanatory Notes* (eds Findlay, R. H., Arumba, J., Kopi, G. & Nekitel, S.) (Geological Survey of Papua New Guinea, in the press).
19. Davies, H. L. *et al. Geo-Marine Lett.* **7,** 143–152 (1987).
20. Abbott, L. D., Silver, E. A. & Galewsky, J. *Tectonics* **13,** 1007–1034 (1994).
21. Angevine, C. L., Heller, P. L. & Paola, C. *AAPG Short Course Note Series No. 32* (American Association Petroleum Geologists, 1990).
22. Katz, B. J., Pheifer, R. N. & Schunk, D. J. *Am. Assoc. Petrol. Geol. Bull.* **72,** 926–931 (1988).
23. Gill, J. B., Morris, J. D. & Johnson, R. W. *Geochim. Cosmochim. Acta* **57,** 4269–4283 (1993).
24. Mitasova, H. & Mitas, L. *Math. Geol.* **25,** 641–655 (1993).
25. Mitasova, H. & Hofierka, J. *Math. Geol.* **25,** 657–669 (1993).
26. Abers, G. A. & McCaffrey, R. *Tectonics* **13,** 227–245 (1994).
27. Galewsky, J., Silver, E. A. & Abbott, L. D. *Eos* **73,** 535 (1992).
28. Hetenyi, M. *Beams on Elastic Foundation* (University of Michigan Press, Michigan, 1946).
29. Abers, G. A. & Roecker, S. W. *J. Geophys. Res.* **96,** 6379–6401 (1991).
30. Quinn, T. M. & Matthews, R. K. *Geology* **18,** 942–945 (1990).
31. Haq, B. U., Hardenbol, J. & Vail, P. R. in *SEPM Spec. Publ. 42* (ed. Wilgus, C. K.) 71–108 (Soc. Economic Paleo. Mineral., 1988).
32. Prentice, M. L. & Matthews, R. K. *Geology* **16,** 963–966 (1988).
33. Crook, K. A. W. *Tectonophysics* **163,** 105–118 (1989).
34. Kulig, C., McCaffrey, R., Abers, G. A. & Letz, H. *Tectonophysics* **227,** 81–93 (1993).
35. Taylor, B. *Geology* **7,** 171–174 (1979).
36. Berggren, W. A. *et al. SEPM Spec. Publ.* **54,** 129–212 (1995).
37. Berggren, W. A. *et al. Geol. Soc. Am. Bull.* **107,** 1272–1287 (1995).
38. Ingle, J. C. *Cushman Foundation Spec. Publ.* **19,** 163–195 (1980).
39. Pettifer, G. R. *Austr. BMR Rec. 174/65* (1974).

Acknowledgements. J. Werlin, S. Nekitel, Hon. G. G. Saonu (MP) and many residents of the Finisterre range assisted with sample colleciton. The manuscript was improved by reviews from D. Burbank and T. Cook. The project was supported by grants from the Earth Sciences Program of the National Science Foundation (E.A.S. and R.S.A.).

Correspondence should be addressed to L.D.A. (e-mail: lon@earthsci.ucsc.edu).